

# Intrathecal delivery of a palmitoylated peptide targeting Y382-384 within the P2X7 receptor alleviates neuropathic pain

Molecular Pain  
Volume 14: 1–10  
© The Author(s) 2018  
Article reuse guidelines:  
sagepub.com/journals-permissions  
DOI: 10.1177/1744806918795793  
journals.sagepub.com/home/mpx  


Rebecca Dalgarno<sup>1,2,3</sup>, Heather Leduc-Pessah<sup>1,2,3</sup>,  
Alexandra Pilapil<sup>1,2,3</sup>, Charlie HT Kwok<sup>1,2,3</sup>, and Tuan Trang<sup>1,2,3</sup> 

## Abstract

Pain hypersensitivity resulting from peripheral nerve injury depends on pathological microglial activation in the dorsal horn of the spinal cord. This microglial activity is critically modulated by P2X7 receptors (P2X7R) and ATP stimulation of these receptors produces mechanical allodynia, a defining feature of neuropathic pain. Peripheral nerve injury increases P2X7R expression and potentiates its cation channel function in spinal microglia. Here, we report a means to preferentially block the potentiation of P2X7R function by delivering a membrane permeant small interfering peptide that targets Y<sub>382-384</sub>, a putative tyrosine phosphorylation site within the P2X7R intracellular C-terminal domain. Intrathecal administration of this palmitoylated peptide (P2X7R<sub>379-389</sub>) transiently reversed mechanical allodynia caused by peripheral nerve injury in both male and female rats. Furthermore, targeting Y<sub>382-384</sub> suppressed P2X7R-mediated release of cytokine tumor necrosis factor alpha and blocked the adoptive transfer of mechanical allodynia caused by intrathecal injection of P2X7R-stimulated microglia. Thus, Y<sub>382-384</sub> site-specific modulation of P2X7R is an important microglial mechanism in neuropathic pain.

## Keywords

Neuropathic pain, microglia, P2X7 receptors, spinal cord

Date Received: 18 May 2018; revised: 22 June 2018; accepted: 9 July 2018

## Introduction

Chronic pain after nerve injury is the consequence of a pathologically altered nervous system.<sup>1,2</sup> Activated microglia are a cellular feature of this altered system, which in the spinal dorsal horn is characterized by aberrant nociceptive output that gives rise to mechanical allodynia, a hallmark symptom of neuropathic pain.<sup>3–5</sup> Several microglial mechanisms contribute to nerve injury-induced mechanical allodynia, with particular attention focused on developing compounds that block ATP-gated P2X7 receptors (P2X7Rs), because of their critical role in inflammatory and neuropathic pain conditions.<sup>6,7</sup> In particular, P2X7Rs expressed on microglia are causally implicated in a variety of chronic pain conditions. P2X7Rs regulate microglial activation, proliferation, and the release of proinflammatory mediators.<sup>8–10</sup> These P2X7R-dependent processes play a key role in the microglial response to peripheral nerve injury, but the

mechanisms that regulate P2X7Rs remain an important open question.

Our group recently identified tyrosine residues Y<sub>382-384</sub> within the P2X7R C-terminal domain as a critical site for regulating microglial P2X7R function in response to morphine treatment.<sup>9</sup> We determined Y<sub>382-384</sub> is a putative phosphorylation site that gates the potentiation of P2X7R cation channel function

<sup>1</sup>Department of Comparative Biology & Experimental Medicine, University of Calgary, Calgary, Alberta, Canada

<sup>2</sup>Department of Physiology & Pharmacology, University of Calgary, Calgary, Alberta, Canada

<sup>3</sup>Hotchkiss Brain Institute, University of Calgary, Calgary, Alberta, Canada  
The first two authors contributed equally to this work.

### Corresponding Author:

Tuan Trang, Department of Comparative Biology & Experimental Medicine, Hotchkiss Brain Institute, University of Calgary, 3330 Hospital Drive, Calgary, Alberta T2N 4N1, Canada.  
Email: trangt@ucalgary.ca



required for the development of morphine analgesic tolerance, and selectively targeting this site dampened spinal microglia activation and preserved the antinociceptive effects of morphine. The requirement for microglial P2X7R is common to both opioid tolerance and neuropathic pain, which share many cellular similarities including a diminished response to the analgesic effects of opioids.<sup>11–14</sup> Given the mechanistic overlap with opioid tolerance, we tested the hypothesis that targeting Y<sub>382–384</sub> may suppress neuropathic pain.

## Methods

### Animals

All experiments were approved by the University of Calgary Animal Care Committee and follow the guidelines of the Canadian Council on Animal Care. Adult male (200–250 g) and female (150–200 g) Sprague-Dawley rats aged 6–8 weeks were purchased from Charles River (Sherbrooke, QC, Canada). Rats were housed under a 12-h light/dark cycle with food and water available ad libitum.

### Spared nerve injury model

The spared nerve injury (SNI) model was performed as previously described.<sup>15</sup> Briefly, rats were anesthetized with 2% isoflurane (Fresenius Kabi, Bad Homburg vor der Höhe, Germany) and an incision was made on the left thigh to expose the sciatic nerve and its three terminal branches (sural, common peroneal, and tibial nerves). The common peroneal and tibial nerves were tightly ligated and transected, while the sural nerve was left intact. The muscle and skin were sutured and the rat was removed from anesthesia while being closely monitored. Sham surgeries were performed as a control, exposing the nerves without ligation and transection.

### Behavioral testing (von Frey)

Rats were acclimatized to handling for three days prior to commencement of behavioral testing and habituated in clear Plexiglas chambers for at least 1 h prior to taking measurements. All experiments were conducted during the light cycle. The SNI model produces marked mechanical hypersensitivity in the lateral area of the paw, which is innervated by the spared sural nerve. In nerve injured rats, mechanical allodynia was assessed by applying a series of von Frey filaments (0.6–26.0 g) (Ugo Basile, Varese, Italy) to the lateral plantar surface of the ipsilateral hind paw. Mechanical thresholds were measured using the modified up-down method.<sup>16</sup> Mechanical threshold was assessed at day 0 (baseline) and at days 3, 5, and 7 following sham or SNI surgeries. In reversal experiments, an intrathecal injection was performed on

day 7 after injury, and the lateral aspect of each hind paw was tested at time 0 (baseline) and at 30, 60, 90, 120, and 150 min post-injection.

### Intrathecal drug administration

Palmitoylated peptides were delivered to the spinal intrathecal space at L3–L5 via lumbar puncture with a 30-gauge needle connected to a Hamilton syringe. Active P2X7R<sub>379–389</sub> (VNEYYYRKKCE) and inactive iP2X7R<sub>379–389</sub> (VNEFFFRKKCE) peptides were synthesized based on P2X7R protein sequences from NCBI (*rattus norvegicus*: NP\_062129.1) by Genemed Synthesis Inc. (San Antonio, TX). Both peptides were conjugated to a palmitoyl group to allow cell membrane permeability. The mimetic peptide P2X7R<sub>379–389</sub> spans the region containing tyrosine residues 382–384 (Y<sub>382–384</sub>) of the P2X7R C-terminal domain. Tyrosine residues were replaced with non-phosphorylatable phenylalanine residues (Y<sub>382–384</sub>F) to create an inactive P2X7R<sub>379–389</sub> peptide. Peptides were reconstituted in phosphate buffered saline (PBS) to a final concentration of 5 μM. A volume of 30 μL was administered for all intrathecal injections.

### Microglia cell cultures

**Primary microglia culture from adult spinal cords.** On day 7 post-surgery, male or female rats were anaesthetized, the spinal cord was isolated by hydraulic extrusion, and the dorsal ipsilateral lumbar region was placed in Hanks Balanced Salt Solution (Life Technologies, Carlsbad, CA). Following blunt dissociation using a Miltex surgical blade, the spinal cord was filtered through a 70-μm cell strainer into Dulbecco's Modified Eagles Medium (DMEM) (Life Technologies) containing 10 mM 4-(2-Hydroxyethyl)piperazine-1-ethanesulfonic acid (HEPES) (Sigma, St. Louis, MO) and 2% fetal bovine serum (FBS) (Life Technologies). Isotonic Percoll (density 1.23 g/mL) (GE Healthcare, Little Chalfont, UK) was added to the cell suspension, followed by a 1.08-g/mL Percoll underlay. Samples were spun at 3000 r/min for 30 min at 20°C. Following centrifugation, myelin debris was removed, and the interface was collected and transferred into fresh medium. Samples were centrifuged again at 1400 r/min for 10 min at 4°C, and the pellet was reconstituted in PBS containing 10% FBS for flow cytometry or DMEM containing 10% FBS and 1% penicillin–streptomycin (Thermo Fisher Scientific, Waltham, MA) for calcium imaging.

**Primary microglia culture from postnatal rats.** Microglia cultures were prepared as previously described by Trang et al.<sup>17</sup> In brief, mixed glial culture was isolated from the brains of male P1–P3 postnatal Sprague-Dawley

rats and maintained for 10–14 days in DMEM containing 10% FBS and 1% Penicillin-Streptomycin at 37°C with 5% carbon dioxide (CO<sub>2</sub>). Microglia were separated from the mixed culture by gentle shaking and replated onto 25 mm coverslips for live-cell imaging or into dishes for treatment and collection for Western blot analysis.

**Calcium imaging.** Primary microglia isolated from adult rat spinal cords were incubated for 30 min with the fluorescent Ca<sup>2+</sup> indicator dye Fura-2 conjugated to acetoxymethyl ester (Fura-2 AM) (2.5 μM; Molecular Probes, Eugene, OR) in extracellular solution (ECS) containing 140 mM NaCl, 5.4 mM KCl, 1.3 mM CaCl<sub>2</sub>, 10 mM HEPES, and 33 mM Glucose (pH 7.35). All experiments were conducted at room temperature using an inverted microscope (Nikon Eclipse Ti C1SI Spectral Confocal, Nikon, Tokyo, Japan) and the fluorescence of individual microglia was recorded using EasyRatioPro software (PTI, London, ON). Excitation light was generated from a xenon arc lamp and passed in alternating manner through 340 or 380 nm bandpass filters (Omega Optical, VT). The 340/380 fluorescence ratio was calculated after baseline subtraction.

**Microglia transfer experiments.** Primary microglia were collected as previously described.<sup>18</sup> Cells were rinsed with ECS, transferred to Eppendorf tubes, and cell concentrations were adjusted to 100 cells/μL in ECS. Primary microglia cultures were treated with ECS or 2'(3')-O-(4-Benzoylbenzoyl)adenosine-5'-triphosphate tri(triethylammonium) salt (BzATP, 100 μM) (Toronto Research Chemicals Inc., North York, ON) for 30 min, or pretreated with 10 μM of P2X7R<sub>379–389</sub> or iP2X7R<sub>379–389</sub> for 15 min prior to stimulation with BzATP or ECS as a control; 30 μL of the sample was immediately injected into the intrathecal space of non-injured naïve male rats. The mechanical threshold was assessed by applying von Frey filaments onto the medial aspect of each hind paw and the resulting values from both paws averaged. Measurements of mechanical threshold were taken at time 0 (baseline) and at 30, 60, 90, 120, 150, 180, 210, and 240 min after intrathecal injection of ECS- or BzATP-stimulated microglia.

### Flow cytometry

Mixed culture was isolated from the ipsilateral spinal dorsal horn of adult rats as described above. Cells were stained as previously described with fluorophore-conjugated CD11b/c-PE (eBioscience, San Diego, CA) and rabbit antibody to extracellular P2X7R preincubated with fluorophore-conjugated anti-rabbit secondary antibody (Alomone, Jerusalem, Israel). Cell fluorescence was measured by an Attune Acoustic Focusing Cytometer (Applied Biosystems, Foster City,

CA). Live single-cell population was gated using forward and side scatter plots. CD11b- and P2X7R-positive staining were gated using BL2 and RL1 intensities, respectively, in single stained cells compared to unstained cells confirming P2X7R and CD11b antibody specificity as previously described.<sup>9</sup>

### Immunohistochemistry

Spinal cords were extracted, post-fixed in formalin overnight, and transferred to 30% sucrose solution at 4°C overnight. The lumbar spinal cord (L3-L5) was sectioned at 30 μm thickness using a cryostat. Spinal sections were washed, blocked with 2% normal goat serum (Sigma) containing 0.3% Triton for 1 h, and incubated overnight at 4°C in mouse α-CD11b antibody (1:150, CBL1512 EMD Millipore, Darmstadt, Germany). Sections were washed in PBS prior to incubation with fluorochrome-conjugated secondary antibody (1:1000, Cy3-conjugated AffiniPure Donkey anti-mouse IgG, Jackson Immuno Research, West Grove, PA, USA) for 2 h at room temperature. Sections were mounted and imaged using Nikon Eclipse Ti (C1SI Spectral Confocal) and A1R multiphoton microscopes. Images were acquired using E2-C1 software and CD11b-IR mean intensity and percent area were quantified using ImageJ software.

### Western blotting

Male and female rats were euthanized 7 days following sham or SNI surgeries and spinal cords collected via hydraulic extrusion. The ipsilateral dorsal horn of the lumbar spinal region was isolated by blunt dissection. Cells were harvested in cell lysis buffer containing 50 mM TrisHCl, 150 mM NaCl, 10 mM EDTA, 0.1% Triton-X, 5% glycerol, protease inhibitors (Sigma), and phosphatase inhibitors (Life Sciences, Saint Louis, MO) and left on ice for 30 min prior to centrifugation at 10,000 r/min at 4°C for 30 min. Total protein was measured using a BCA Protein Assay Kit (Thermo Scientific). Samples were heated at 95°C for 5 min in loading buffer (350 mM Tris, 30% glycerol, 1.6% SDS, 1.2% bromophenol blue, 10% β-mercaptoethanol (Sigma)), electrophoresed on a 12% gel, and transferred onto a nitrocellulose membrane. The membrane was blocked with 5% milk for 1 h prior to overnight incubation with antibody targeting β-actin (1:2000, Sigma) and tumor necrosis factor alpha (TNFα) (1:1000, Abcam, Cambridge, UK). Membranes were washed with TBST and incubated for 1 h at room temperature in anti-mouse and anti-rabbit fluorophore-conjugated secondary antibodies (1:5000, Mandel Scientific, Guelph, ON) and then imaged using the LICOR Odyssey CLx Infrared imaging system. Band intensity was quantified using ImageJ.

### ELISA-based measurement of TNF $\alpha$ release

Primary microglia cultures were collected as previously described<sup>3,17</sup> into eppendorf tubes containing 50  $\mu$ L of ECS. Cells were treated with P2X7R or iP2X7R (10  $\mu$ M) for 30 min prior to stimulation with BzATP (100  $\mu$ M) (Sigma) or ECS for 30 min. Following stimulation, samples were centrifuged at 1500 r/min for 5 min at 4°C; the resulting pellet and supernatant were isolated and stored at -20°C. Measurement of TNF $\alpha$  in the supernatant was performed using a rat TNF $\alpha$  ELISA kit (R&D Systems, Minneapolis, MN) according to the manufacturer's instructions. Samples were considered TNF $\alpha$ -positive if their signal was higher than the background signal and within the range of the standard curve.

### Quantitative polymerase chain reaction

Primary microglia in culture were collected and treated as described above. Extraction of total mRNA from primary microglia was performed using the phenol chloroform method. Cells were collected in Trizol (Thermo Scientific) and lysed using QIAshredder homogenizers (Qiagen, Hilden, Germany). Samples were precipitated with isopropanol (Sigma), washed in 75% ethanol (Sigma), and reconstituted in Tris-EDTA buffer solution (Qiagen). cDNA was generated from the mRNA using reverse transcriptase (Thermo Fisher). Quantitative RT-PCR (polymerase chain reaction) was performed using SsoAdvanced Universal SYBR Green Supermix (BioRad, Hercules, CA) in a real-time PCR system (StepOne Plus, Applied Biosystems). Data were analyzed using the comparative Ct method ( $2^{-\Delta\Delta C_t}$ ) and expression levels were normalized to the values for RPLP RNA. Primer pairs are as follows:

RPLP: 5'-TACCTGCTCAGAACACCGGTCT-3' (forward)  
 RPLP: 5'-GCACATCGCTCAGGATTTCAA-3' (reverse)  
 TNF $\alpha$ : 5'-CATCCGTTCTCTACCCAGCC-3' (forward)  
 TNF $\alpha$ : 5'-AATTCTGAGCCCGGAGTTGG-3' (reverse)

### Statistics

All data are shown as mean  $\pm$  standard error of the mean. Statistical analysis was performed in GraphPad Prism 6 software using unpaired t-test, one-way analysis of variance (ANOVA) (Sidak's post-hoc test), two-way ANOVA (Sidak's or Tukey's post-hoc test), or two-way repeated measures ANOVA (Sidak's post-hoc test). *p* values less than 0.05 were considered significant with significance reported as follows: \**p* < 0.05; \*\**p* < 0.01; \*\*\**p* < 0.001. Exact *p*-values are reported within the figure legends.

### Results

We investigated whether Y<sub>382-384</sub> within the P2X7R contributes to mechanical allodynia using a rat model of SNI.<sup>15</sup> Both male and female rats with SNI, but not sham controls, displayed a marked reduction in mechanical paw withdrawal threshold (Figure 1(a) and (e)). At day 7 after nerve injury, there was a notable increase in CD11b-staining within the ipsilateral spinal dorsal horn in both sexes (Figure 1(b) and (f)). Flow cytometry was used to further discriminate between CD11b-positive (microglia) and CD11b-negative (neurons, astrocytes, oligodendrocytes) cells in the spinal lumbar cord. These two cell populations were co-labeled for P2X7R: In CD11b-expressing cells, P2X7R mean fluorescence intensity (per cell) was significantly increased following peripheral nerve injury as compared with sham control rats. By contrast, nerve injury had no impact on P2X7R fluorescence in CD11b-negative cells (Figure 1(c) and (g)).

To assess P2X7R function, microglia were acutely isolated from the ipsilateral spinal dorsal horn of rats on day 7 after peripheral nerve injury or sham surgery. Spinal microglia were loaded with fura-2, a Ca<sup>2+</sup>-indicator dye, and stimulated with BzATP (100  $\mu$ M), a potent P2X7R agonist. We found that BzATP-evoked Ca<sup>2+</sup> responses were significantly greater in spinal microglia isolated from nerve-injured as compared with sham control rats (Figure 1(d) and (h)). This potentiation of P2X7R function occurred in both male- and female-derived spinal microglia.

Increased P2X7R function is a cellular feature of opioid tolerance and neuropathic pain, and since Y<sub>382-384</sub> gates morphine potentiation of P2X7R function in microglia, we questioned whether this site might also modulate P2X7R response to peripheral nerve injury.<sup>9</sup> To examine this possibility, we used a membrane-permeant palmitoylated peptide corresponding to the 379-389 amino acid region within the P2X7R C-terminus (P2X7R<sub>379-389</sub>): This peptide interferes with signaling at Y<sub>382-384</sub>, a putative tyrosine phosphorylation site.<sup>9</sup> Spinal microglia acutely isolated from male or female nerve-injured rats were treated in culture with the P2X7R<sub>379-389</sub> peptide prior to BzATP stimulation. In the presence of P2X7R<sub>379-389</sub>, BzATP-evoked Ca<sup>2+</sup> responses were indistinguishable in microglia isolated from SNI vs. sham control rats (Figure 2(a) and (d)). P2X7R<sub>379-389</sub> peptide had no effect on BzATP-evoked Ca<sup>2+</sup> responses in sham control rats (Sham: *n* = 60, mean = 0.99  $\pm$  0.04; Sham/P2X7R<sub>379-389</sub>: *n* = 26, mean = 1.01  $\pm$  0.06, Unpaired t-test, no significance, *t*<sub>84</sub> = 0.2541). Targeting Y<sub>382-384</sub> therefore blocked the potentiation of P2X7R-mediated Ca<sup>2+</sup> responses, without affecting normal cation channel function. As a control, we used an inactive palmitoylated peptide

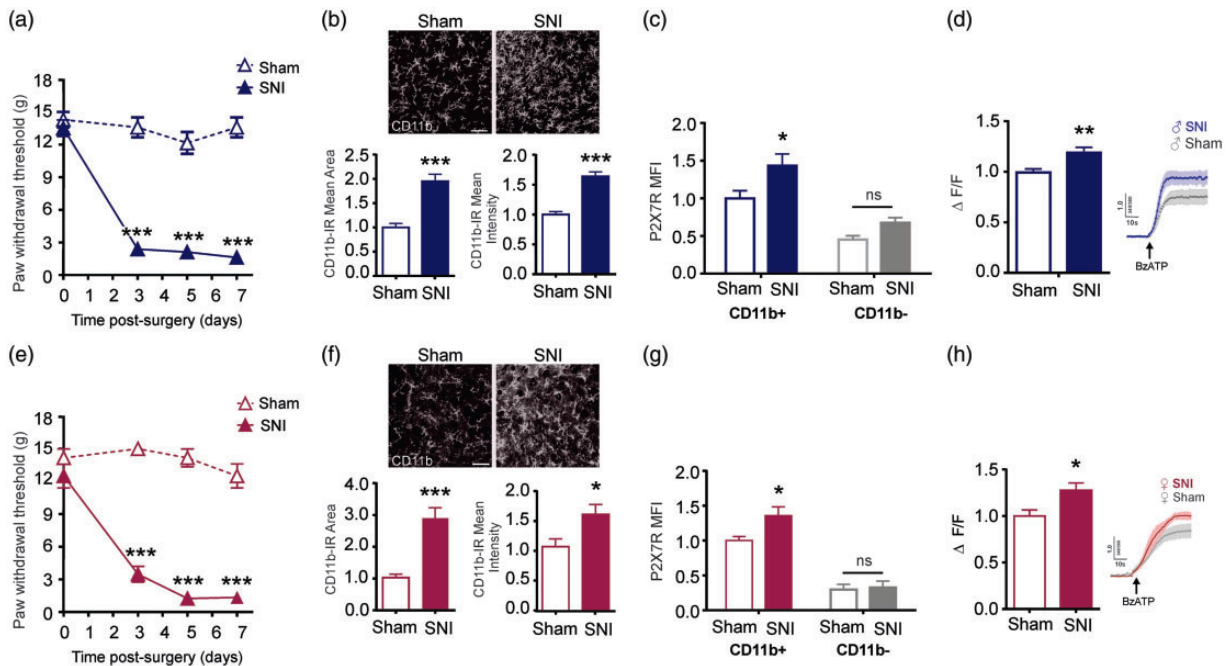


**Figure 1.** Peripheral nerve injury increases P2X7R function in spinal microglia. (a) Time course of mechanical paw withdrawal thresholds measured using von Frey filament testing at baseline (day 0) and on days 3, 5, and 7 following sham (N=7) or SNI surgeries (N=10) in male rats. \* represents SNI compared to sham on each day post-surgery. Two-way repeated measures ANOVA (effect of surgery,  $F_{1, 15} = 175.15$ ,  $p < 0.001$ ). (b) Representative images of CD11b staining in spinal dorsal horn seven days following sham or nerve injury in male rats (N=12 rats per group). Quantification of CD11b immunoreactivity (IR) mean area and mean intensity of staining. Data are shown relative to sham controls. Scale bar = 50  $\mu\text{m}$ . Unpaired t-test for IR mean area ( $t_{5,782} = 22$ ,  $p < 0.001$ ). Unpaired t-test for IR mean intensity ( $t_{6,988} = 22$ ,  $p < 0.001$ ). (c) Flow cytometric analysis of P2X7R mean fluorescence intensity (MFI) per cell in CD11b+ and CD11b- populations isolated from the ipsilateral spinal dorsal horn seven days post sham or SNI surgeries in male rats (N=7 experimental replicates from 6 rats per group). Data are normalized to CD11b+ sham control. \* represents SNI compared to sham. Two-way ANOVA (effect of surgery,  $F_{1, 24} = 10.06$ ,  $p = 0.0041$ ; effect of CD11b+,  $F_{1, 24} = 40.09$ ,  $p < 0.001$ ). (d) Left: Average  $\Delta F/F$  of single-cell calcium responses evoked by BzATP (100  $\mu\text{M}$ ) in microglia isolated from the ipsilateral spinal dorsal horn of male rats seven days following sham (N=60 cells from 9 rats) or SNI (N=50 cells from 9 rats). Data are normalized to sham control. Right: Representative BzATP-evoked  $\text{Ca}^{2+}$  traces (average of three). Unpaired t-test ( $t_{3,13} = 108$ ,  $p = 0.0023$ ). (e) Time course of mechanical paw withdrawal thresholds measured using von Frey filament testing at baseline (day 0) and on days 3, 5, and 7 following sham or SNI surgeries in female rats (N= 6 rats per group). \* represents SNI compared to sham on each day post-surgery. Two-way repeated measures ANOVA (effect of surgery,  $F_{1, 10} = 143.96$ ,  $p < 0.001$ ). (f) Representative images of CD11b staining in spinal dorsal horn seven days following sham (N=5) or nerve injury (N=6) in female rats. Quantification of CD11b IR mean area and mean intensity of staining. Data are shown relative to sham controls. Scale bar = 50  $\mu\text{m}$ . Unpaired t-test for IR mean area ( $t_{5,012} = 9$ ,  $p = 0.0007$ ). Unpaired t-test for IR mean intensity ( $t_{2,5} = 9$ ,  $p = 0.0339$ ). (g) Flow cytometric analysis of mean P2X7R Fluorescence in CD11b+ and CD11b- populations of cells isolated from the ipsilateral spinal dorsal horn of rats seven days post sham or SNI surgeries in female rats (N=6 experimental replicates from 6 rats per group). Data are normalized to CD11b+ sham control. \* represents SNI compared to sham. Two-way ANOVA (effect of surgery,  $F_{1, 20} = 4.47$ ,  $p = 0.0472$ ; effect of CD11b+,  $F_{1, 20} = 89.61$ ,  $p < 0.001$ ). (h) Left: Average  $\Delta F/F$  of single-cell calcium responses evoked by BzATP (100  $\mu\text{M}$ ) in microglia isolated from the ipsilateral spinal dorsal horn of female rats seven days following sham (N=54 cells from 6 rats) or SNI (N=25 cells from 8 rats). Right: representative BzATP-evoked  $\text{Ca}^{2+}$  traces (average of four). Unpaired t-test ( $t_{2,497} = 77$ ,  $p = 0.0147$ ). All data represent mean  $\pm$  SEM. \* $p < 0.05$ ; \*\* $p < 0.01$ ; \*\*\* $p < 0.001$ . SNI: spared nerve injury.

(iP2X7R<sub>379-389</sub>) in which tyrosine residues 382-384 were substituted with non-phosphorylatable phenylalanine residues (Y<sub>382-384</sub>F). The control peptide had no effect on the increased P2X7R activity in microglia isolated from nerve-injured rats (Figure 2(a) and (d)).

We next examined whether targeting the Y<sub>382-384</sub> site affects mechanical allodynia at day 7 after nerve injury. In both male and female nerve-injured rats, an intrathecal injection of the P2X7R<sub>379-389</sub> mimetic peptide but not

inactive peptide transiently reversed mechanical allodynia. This reversal was reflected by an increase in mechanical paw withdrawal threshold that peaked 90 min after the injection (Figure 2(b) and (e)). When either peptide was administered to naïve (non-injured) rats, there was no impact on basal mechanical threshold (Figure 2(c)). Together, our results indicate that Y<sub>382-384</sub> is required for the potentiation of P2X7R activity in microglia, and targeting this site alleviates mechanical allodynia

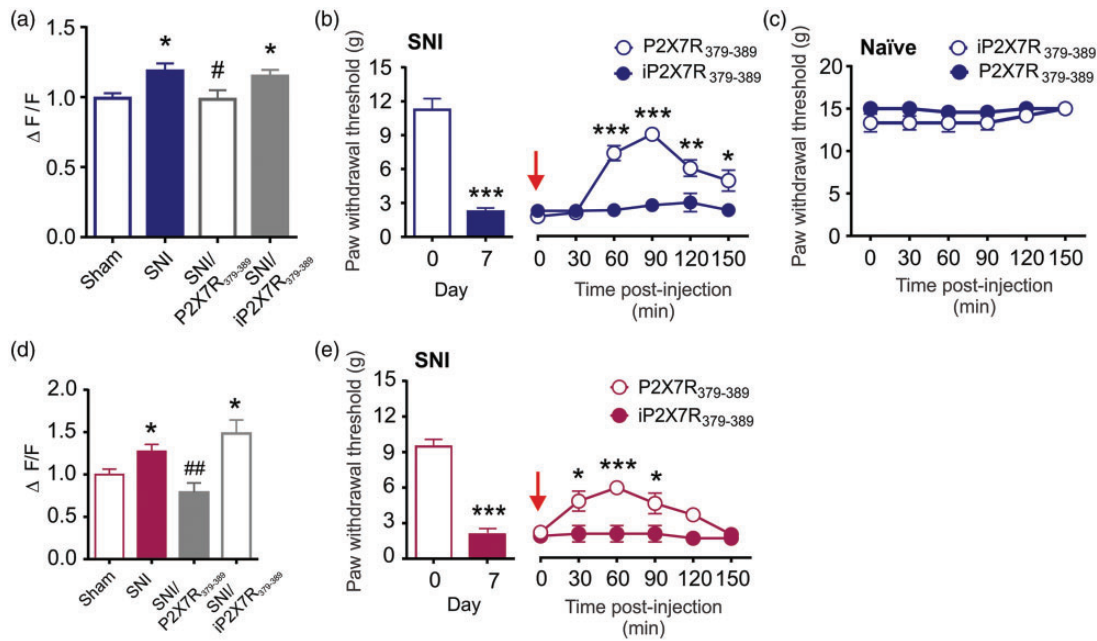


**Figure 2.** Y<sub>382-384</sub> is critical for potentiation of microglial P2X7R function and the maintenance of allodynia following peripheral nerve injury. (a) Quantification of BzATP-evoked calcium responses measured in spinal microglia isolated seven days following sham or nerve injury in male rats. Cells were pretreated with ECS (Sham N=50 cells; SNI N=60 cells), P2X7R<sub>379-389</sub> (N=33 cells), or inactive P2X7R<sub>379-389</sub> (N=67 cells) at 10 μM for 90 min prior to stimulation with BzATP (100 μM). Sham and SNI groups are the same as shown in Figure 1 (d). Data are shown relative to sham control. \* represents comparison with Sham; # represents comparison with SNI. One-way ANOVA ( $F_{3, 206} = 4.564, p = 0.0041$ ). (b) Left: Mechanical paw withdrawal thresholds on day 7 post-sham or SNI surgeries in male rats (N=12 rats per group); Unpaired t-test ( $t_{9,06} = 22, p < 0.001$ ). Right: Effects of intrathecal administration of 5 μM active (P2X7R<sub>379-389</sub>) or inactive peptide (iP2X7R<sub>379-389</sub>) on paw withdrawal thresholds over 150 min in nerve-injured male rats (N=6 rats per group). \* represents P2X7R<sub>379-389</sub> compared to iP2X7R<sub>379-389</sub> at each timepoint. Two-way repeated measures ANOVA (effect of treatment,  $F_{1,10} = 14.42, p = 0.0035$ ). (c) Paw withdrawal thresholds following intrathecal administration of P2X7R<sub>379-389</sub> or iP2X7R<sub>379-389</sub> in naive rats over 150 min (N=6 rats per group). (d) Quantification of BzATP-evoked calcium responses measured in spinal microglia isolated seven days following sham or nerve injury in female rats. Cells were pretreated with ECS (Sham N=54 cells; SNI N=25 cells), P2X7R<sub>379-389</sub> (N=14 cells), or inactive P2X7R<sub>379-389</sub> (N=9 cells) at 10 μM for 90 min prior to stimulation with BzATP (100 μM). Sham and SNI groups are the same as shown in Figure 1 (h). Data are shown relative to sham control. \* represents comparison with Sham; # represents comparison with SNI. One-way ANOVA ( $F_{3, 98} = 6.46, p = 0.0005$ ). (e) Left: Mechanical paw withdrawal thresholds on day 7 post-sham or SNI surgeries in female rats. (N=10 rats per group); Unpaired t-test ( $t_{10,93} = 18, p < 0.001$ ). Right: Effects of intrathecal administration of 5 μM active (P2X7R<sub>379-389</sub>) or inactive peptide (iP2X7R<sub>379-389</sub>) on paw withdrawal thresholds over 150 min in nerve-injured female rats (N=5 rats per group). \* represents P2X7R<sub>379-389</sub> compared to iP2X7R<sub>379-389</sub> at each timepoint. Two-way repeated measures ANOVA (effect of treatment,  $F_{1,8} = 10.92, p = 0.0108$ ). All data represent mean ± SEM. \* $p < 0.05$ ; \*\* $p < 0.01$ ; \*\*\* $p < 0.001$ ; # $p < 0.05$ ; ## $p < 0.01$ . SNI: spared nerve injury.

following peripheral nerve injury. Furthermore, the regulation of P2X7R activity by Y<sub>382-384</sub> in response to nerve injury is not sex-dependent.

To test whether activation of P2X7Rs in microglia is sufficient to produce mechanical allodynia, we administered BzATP-stimulated microglia to the lumbar spinal level of naive rats by intrathecal injection. Mechanical paw withdrawal threshold significantly decreased after the intrathecal injection of BzATP-stimulated microglia (Figure 3(a)). This reduction in mechanical threshold was prevented by the P2X7R<sub>379-389</sub> mimetic peptide, but not by the inactive iP2X7R<sub>379-389</sub> peptide (Figure 3(b)). By contrast, intrathecal injection of unstimulated microglia had no effect on mechanical

paw withdrawal threshold (Figure 3(b)). P2X7R-stimulated microglia are therefore sufficient to produce tactile allodynia that is blocked by targeting Y<sub>382-384</sub>.

P2X7R activation critically modulates cytokine expression and release in microglia.<sup>19–21</sup> In the ipsilateral spinal dorsal horn, tumour necrosis factor alpha (TNFα) protein expression was increased following SNI (Figure 4 (a)). In primary microglia culture, exposure to BzATP significantly increased TNFα mRNA (Figure 4(b)) and elevated TNFα levels in the microglial supernatant (Figure 4(c)); both of these responses were blocked by treatment with the P2X7R<sub>379-389</sub> peptide. These findings indicate that Y<sub>382-384</sub> within the P2X7R modulates the transcription and release of TNFα in microglia.

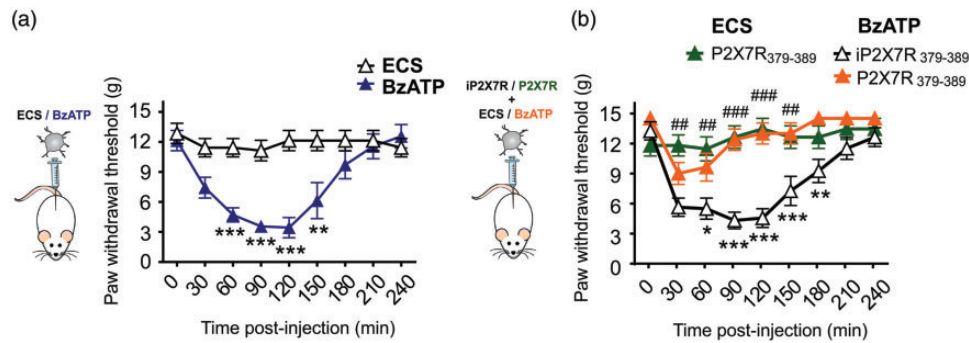


**Figure 3.** Y<sub>382-384</sub> targeting peptide blocks mechanical allodynia caused by adoptive transfer of P2X7R-stimulated microglia. Paw withdrawal thresholds were measured at 30 min timepoints over 240 min following adoptive transfer of primary postnatal microglia. (a) Primary postnatal microglia were treated with ECS or BzATP (100  $\mu$ M) for 30 min prior to intrathecal administration (N=7 per group). \*represents comparison of ECS to BzATP-treated cells at each timepoint. Two-way repeated measures ANOVA (effect of treatment,  $F_{1,12} = 13.56$ ,  $p = 0.0031$ ). (b) Primary postnatal microglia were treated with P2X7R<sub>379-389</sub> or inactive P2X7R<sub>379-389</sub> peptide (10  $\mu$ M) for 30 min prior to application of BzATP (100  $\mu$ M) (N=8 per group) or ECS (N=6 per group) for 30 min. \*represents comparison between BzATP/IP2X7R<sub>379-389</sub> and BzATP/P2X7R<sub>379-389</sub> at each timepoint. Two-way repeated measures ANOVA (effect of treatment,  $F_{1,14} = 27.41$ ,  $p = 0.0001$ ). #represents comparison between ECS/P2X7R<sub>379-389</sub> and BzATP/P2X7R<sub>379-389</sub> at each timepoint. Two-way repeated measures ANOVA (effect of treatment,  $F_{1,12} = 19.02$ ,  $p = 0.0009$ ). All data represent mean  $\pm$  SEM. \* $p < 0.05$ ; \*\* $p < 0.01$ ; \*\*\* $p < 0.001$ , ### $p < 0.01$ ; #### $p < 0.001$ . ECS: extracellular solution; BzATP: 2'(3')-O-(4-Benzoylbenzoyl)adenosine-5'-triphosphate tri(triethylammonium) salt.

## Discussion

Peripheral nerve injury causes a pathological amplification of sensory processing in the spinal cord that underlies the exaggerated pain responses associated with neuropathic pain and other chronic pain conditions.<sup>15,22</sup> This pathologically altered system arises because of the release of several mediators. In particular, ATP release is a requisite step that drives the microglial response to nerve injury.<sup>23–25</sup> In the spinal cord, a principal source of this ATP is from intrinsic spinal dorsal horn neurons.<sup>23</sup> ATP can also derive from microglia, which express ATP-gated P2X4R and P2X7R that are causally implicated in the sequelae of neuropathic pain.<sup>26,27</sup> Here, we focused on the P2X7R because of its importance in regulating microglial proliferation, activation, and signaling.<sup>10,25</sup> We showed that peripheral nerve injury increased P2X7R expression and function in microglia: The increase in P2X7R function was dependent upon Y<sub>382-384</sub>, a putative tyrosine phosphorylation site.<sup>9</sup> Interfering with Y<sub>382-384</sub> suppressed the potentiation of P2X7R function in spinal microglia and alleviated mechanical allodynia in male and female rats following peripheral nerve injury. Although sex-specific microglial mechanisms have been implicated in neuropathic pain,<sup>28,29</sup> our results indicate that Y<sub>382-384</sub> modulation of P2X7R function in response to nerve injury is a convergent sex-independent microglial mechanism.

Several tyrosine residues are contained within the P2X7R intracellular C-terminal domain, a key region that regulates P2X7R trafficking, internalization, and function.<sup>30–32</sup> Tyrosine residues are a common target

for post-translational phosphorylation, which can mediate receptor activity through a variety of mechanisms including altered agonist binding, conformational changes, or downstream signaling. Phosphorylation of the P2X7R at other sites has been previously reported to alter receptor function.<sup>33</sup> More recently, we identified Y<sub>382-384</sub> as a putative tyrosine phosphorylation site that gates P2X7R cation channel function in a Src kinase-dependent fashion. This site differentially modulates P2X7R function without impacting the intracellular or cell surface expression of P2X7R in microglia.<sup>9</sup> Therefore, an alternative explanation is that phosphorylation of Y<sub>382-384</sub> may gate P2X7R function by changing receptor conformation, channel opening, and/or agonist-receptor binding. This phosphorylation could occur directly on the P2X7R or indirectly on proteins associated with the P2X7R complex, altering the protein–protein interactions required for increased P2X7R function. We identified Src as the protein tyrosine kinase responsible for phosphorylation of P2X7R in microglia.<sup>9</sup> Indeed, Src activation in spinal microglia is a known consequence of peripheral nerve injury and inhibition of this kinase in animal models of nerve injury and cancer-induced bone pain attenuates neuropathic pain.<sup>34–36</sup> Although the sequence surrounding Y<sub>382-384</sub> does not conform to a known Src phosphorylation consensus sequence, there are many examples of receptors and proteins that do not contain a canonical Src binding sequence but yet are targets of Src kinase activity.<sup>37,38</sup>

P2X7R activation drives the release of pro-inflammatory cytokines, chemokines, and a host of other signaling molecules.<sup>39–42</sup> This release is a core

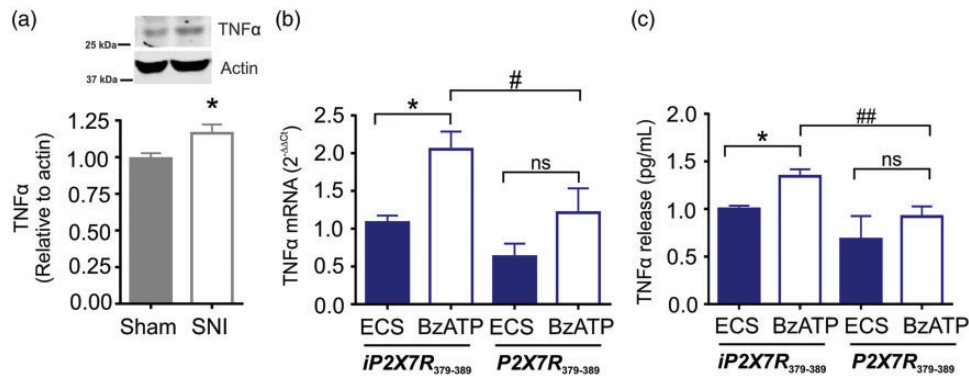


**Figure 4.**  $Y_{382-384}$  modulates  $TNF\alpha$  release from P2X7R-stimulated primary microglia. (a)  $TNF\alpha$  protein levels measured by Western blot in the ipsilateral spinal dorsal horn on day 7 following sham or SNI surgeries (N=14 rats per group). Data are shown relative to sham control. Unpaired t-test ( $t_{2,479} = 26$ ,  $p = 0.0200$ ). (b)  $TNF\alpha$  mRNA levels were measured by qPCR and quantified using the  $\Delta\Delta C_t$  method in primary postnatal cultures treated with  $iP2X7R_{379-389}$  (ECS N=7; BzATP N=11) or  $P2X7R_{379-389}$  (ECS N=5; BzATP N=8) at  $10 \mu M$  for 30 min prior to BzATP ( $100 \mu M$ ) or ECS administration for 30 min. Data are shown relative to ECS  $iP2X7R_{379-389}$  group. \* represents comparison to ECS control. # represents comparison between BzATP/ $iP2X7R_{379-389}$  and BzATP/ $P2X7R_{379-389}$  group. One-way ANOVA ( $F_{3,27} = 6.033$ ,  $p = 0.0028$ ). (c)  $TNF\alpha$  levels in the supernatant were measured by ELISA in primary postnatal cultures treated with  $iP2X7R_{379-389}$  (ECS N=10; BzATP N=15) or  $P2X7R_{379-389}$  (ECS N=5; BzATP N=11) at  $10 \mu M$  for 30 min prior to BzATP ( $100 \mu M$ ) or ECS administration for 30 min. \* represents comparison to ECS control. # represents comparison between BzATP/ $iP2X7R_{379-389}$  and BzATP/ $P2X7R_{379-389}$  group. One-way ANOVA ( $F_{3,37} = 7.27$ ,  $p = 0.0006$ ). All data represent mean  $\pm$  SEM. \* $p < 0.05$ ; # $p < 0.05$ ; ## $p < 0.01$ ; ns – no significance.  $TNF\alpha$ : tumor necrosis factor alpha; SNI: spared nerve injury; ECS: extracellular solution; BzATP: 2'(3')-O-(4-Benzoylbenzoyl)adenosine-5'-triphosphate tri(triethylammonium) salt.

mechanism by which microglia signal to increase the nociceptive output of spinal dorsal horn neurons.<sup>43–45</sup> Our data in microglia culture suggest that P2X7R activation causes the release and transcription of  $TNF\alpha$ , a pro-inflammatory cytokine with both autocrine and paracrine mechanisms of action.  $TNF\alpha$  signaling has been shown to contribute to the aberrant nociceptive drive observed in the spinal cord after peripheral nerve injury.<sup>46</sup> Interfering with  $Y_{382-384}$  suppressed the increase in  $TNF\alpha$  mRNA. Thus,  $Y_{382-384}$  differentially modulates microglial  $TNF\alpha$  release and transcription in response to P2X7R activation.

A key concept emerging from our study is that targeting  $Y_{382-384}$  prevents the potentiation of P2X7R function caused by peripheral nerve injury without affecting normal BzATP-evoked  $Ca^{2+}$  responses in spinal microglia. This differential regulation of P2X7R is supported by site-directed mutagenesis experiments, wherein P2X7R-mediated currents and  $Ca^{2+}$  responses remain intact despite substituting tyrosine residues 382–384 with non-phosphorylatable alanine residues.<sup>9</sup> Morphine-induced potentiation of P2X7R function, however, was abolished in the  $Y_{382-384A}$  P2X7R mutant.<sup>9</sup> Targeting the unique functional selectivity conferred by  $Y_{382-384}$  could be an important consideration in designing P2X7R-based therapies for treating neuropathic pain, because it allows for the preferential inhibition of mechanisms that upregulated P2X7R function. Therefore, a therapeutic strategy directed against  $Y_{382-384}$  may reduce the risk of side effects produced by indiscriminately blocking P2X7R function.

## Declaration of Conflicting Interests

The author(s) declared no potential conflicts of interest with respect to the research, authorship, and/or publication of this article.

## Funding

The author(s) disclosed receipt of the following financial support for the research, authorship, and/or publication of this article: This work was supported by grants to TT from the Natural Sciences and Engineering Research Council of Canada (NSERC RGPIN418299), the Canadian Institutes of Health Research (CIHR MOP133523), and the Vi Riddell Program for Pediatric Pain. RD and AP were funded by CIHR graduate scholarships, and HLP by an Alberta Innovates Health Solutions Graduate Scholarship.

## ORCID iD

Tuan Trang  <http://orcid.org/0000-0003-3309-9492>

## References

- Costigan M, Scholz J and Woolf C J. Neuropathic pain: a maladaptive response of the nervous system to damage. *Annu Rev Neurosci* 2009; 32: 1–32.
- Coull JAM, Boudreau D, Bachand K, Prescott SA, Nault F, S k A, De Koninck P and De Koninck Y. Trans-synaptic shift in anion gradient in spinal lamina I neurons as a mechanism of neuropathic pain. *Nature* 2003; 424: 938–942.
- Coull JAM, Beggs S, Boudreau D, Boivin D, Tsuda M, Inoue K, Gravel C, Salter MW and De Koninck Y.

- BDNF from microglia causes the shift in neuronal anion gradient underlying neuropathic pain. *Nature* 2005; 438: 1017–1021.
- Echeverry S, Shi XQ, Yang M, Huang H, Wu Y, Chen, Lorenzo L-E, Perez-Sanchez J, Bonin RP, De Koninck Y and Zhang J. Spinal microglia are required for long-term maintenance of neuropathic pain. *Pain* 2017; 158: 1792–1801.
  - Tsuda M, Inoue K and Salter MW. Neuropathic pain and spinal microglia: a big problem from molecules in ‘small’ glia. *Trends Neurosci* 2005; 28: 101–107.
  - Chessell IP, Hatcher JP, Bountra C, Michel AD, Hughes JP, Green P, Egerton J, Murfin M, Richardson J, Peck WL, Grahames CBA, Casula MA, Yiangou Y, Birch R, Anand P and Buell GN. Disruption of the P2X7 purinoceptor gene abolishes chronic inflammatory and neuropathic pain. *Pain* 2005; 114: 386–396.
  - Honore P, Donnelly-Roberts D, Namovic MT, Hsieh G, Zhu CZ, Mikusa JP, Hernandez G, Zhong C, Gauvin DM, Chandran P, Harris R, Medrano AP, Carroll W, Marsh K, Sullivan JP, Faltynek CR and Jarvis MF. A-740003 [N-(1-((cyanoimino)(5-quinolinylamino) methyl)amino)-2,2-dimethylpropyl)-2-(3,4-dimethoxyphenyl)acetamide], a novel and selective P2X7 receptor antagonist, dose-dependently reduces neuropathic pain in the rat. *J Pharmacol Exp Ther* 2006; 319: 1376–1385.
  - Bhattacharya A and Biber K. The microglial ATP-gated ion channel P2X7 as a CNS drug target. *Glia* 2016; 64: 1772–1787.
  - Leduc-Pessah H, Weilinger NL, Fan CY, Burma NE, Thompson RJ and Trang T. Site-specific regulation of P2X7 receptor function in microglia gates morphine analgesic tolerance. *J Neurosci* 2017; 37: 10154–10172. doi:10.1523/JNEUROSCI.0852-17.2017
  - Monif M, Reid CA, Powell KL, Smart ML and Williams DA. The P2X7 receptor drives microglial activation and proliferation: a trophic role for P2X7R pore. *J Neurosci* 2009; 29: 3781–3791.
  - Elman I and Borsook D. Common brain mechanisms of chronic pain and addiction. *Neuron* 2016; 89: 11–36.
  - Mayer DJ, Mao J, Holt J and Price DD. Cellular mechanisms of neuropathic pain, morphine tolerance, and their interactions. *Proc Natl Acad Sci USA* 1999; 96: 7731–7736.
  - Smith HS. Opioids and neuropathic pain. *Pain Physician* 2012; 15: ES93–E110.
  - Trang T, Al-Hasani R, Salvemini D, Salter MW, Gutstein H and Cahill CM. Pain and poppies: the good, the bad, and the ugly of opioid analgesics. *J Neurosci* 2015; 35: 13879–13888.
  - Decosterd I and Woolf CJ. Spared nerve injury: an animal model of persistent peripheral neuropathic pain. *Pain* 2000; 87: 149–158.
  - Chaplan SR, Bach FW, Pogrel JW, Chung JM and Yaksh TL. Quantitative assessment of tactile allodynia in the rat paw. *J Neurosci Methods* 1994; 53: 55–63.
  - Trang T, Beggs S, Wan X and Salter MW. P2X4-receptor mediated synthesis and release of brain-derived neurotrophic factor in microglia is dependent on calcium and p38-mitogen-activated protein kinase activation. *J Neurosci Off J Soc Neurosci* 2009; 29: 3518–3528.
  - Ferrini F, Trang T, Mattioli TA, Laffray S, Del’Guidice T, Lorenzo LE, Castonguay A, Doyon N, Zhang W, Godin AG, Mohr D, Beggs S, Vandal K, Beaulieu JM, Cahill CM, Salter MW and De Koninck Y. Morphine hyperalgesia gated through microglia-mediated disruption of neuronal Cl<sup>-</sup> homeostasis. *Nat Neurosci* 2013; 16: 183–192.
  - He Y, Taylor N, Fourgeaud L and Bhattacharya A. The role of microglial P2X7: modulation of cell death and cytokine release. *J Neuroinflammation* 2017; 14: 135.
  - Monif M, Burnstock G and Williams DA. Microglia: proliferation and activation driven by the P2X7 receptor. *Int J Biochem Cell Biol* 2010; 42: 1753–1756.
  - Shieh C-H, Heinrich A, Serchov T, van Calker D and Biber K. P2X7-dependent, but differentially regulated release of IL-6, CCL2, and TNF- $\alpha$  in cultured mouse microglia. *Glia* 2014; 62: 592–607.
  - Latremoliere A and Woolf CJ. Central sensitization: a generator of pain hypersensitivity by central neural plasticity. *J Pain* 2009; 10: 895–926.
  - Masuda T, Ozono Y, Mikuriya S, Kohro Y, Tozaki-Saitoh H, Iwatsuki K, Uneyama H, Ichikawa R, Salter MW, Tsuda M and Inoue K. Dorsal horn neurons release extracellular ATP in a VNUT-dependent manner that underlies neuropathic pain. *Nat Commun* 2016; 7: 12529.
  - Samuels SE, Lipitz JB, Dahl G and Muller KJ. Neuroglial ATP release through innexin channels controls microglial cell movement to a nerve injury. *J Gen Physiol* 2010; 136: 425–442.
  - Trang T, Beggs S and Salter MW. ATP receptors gate microglia signaling in neuropathic pain. *Exp Neurol* 2012; 234: 354–361.
  - Kato Y, Hiasa M, Ichikawa R, Hasuzawa N, Kadowaki A, Iwatsuki K, Shima K, Endo Y, Kitahara Y, Inoue T, Nomura M, Omote H, Moriyama Y and Miyaji T. Identification of a vesicular ATP release inhibitor for the treatment of neuropathic and inflammatory pain. *Proc Natl Acad Sci U S A* Epub ahead of print 2017. doi:10.1073/pnas.1704847114
  - Moriyama Y and Nomura M. Clodronate: a vesicular ATP release blocker. *Trends Pharmacol Sci* 2018; 39: 13–23.
  - Sorge RE, Mapplebeck JCS, Rosen S, Beggs S, Taves S, Alexander JK, Martin LJ, Austin J-S, Sotocinal SG, Chen D, Yang M, Shi XQ, Huang H, Pillion NJ, Bilan PJ, Tu Y Shan, Klip A, Ji R-R, Zhang J, Salter MW and Mogil JS. Different immune cells mediate mechanical pain hypersensitivity in male and female mice. *Nat Neurosci* 2015; 18: 1081–1083.
  - Taves S, Berta T, Liu D-L, Gan S, Chen G, Kim YH, Van de Ven T, Laufer S and Ji R-R. Spinal inhibition of p38 MAP kinase reduces inflammatory and neuropathic pain in male but not female mice: sex-dependent microglial signaling in the spinal cord. *Brain Behav Immun* 2016; 55: 70–81.
  - Costa-Junior HM, Sarmiento Vieira F and Coutinho-Silva R. C terminus of the P2X7 receptor: treasure hunting. *Purinergic Signal* 2011; 7: 7–19.
  - Kim M, Jiang LH, Wilson HL, North RA and Surprenant A. Proteomic and functional evidence for a P2X7 receptor signalling complex. *Embo J* 2001; 20: 6347–6358.

32. Surprenant A, Rassendren F, Kawashima E, North RA and Buell G. The cytolytic P2Z receptor for extracellular ATP identified as a P2X receptor (P2X7). *Science* 1996; 272: 735–738.
33. Adinolfi E, Kim M, Young MT, Di Virgilio F and Surprenant A. Tyrosine phosphorylation of HSP90 within the P2X7 receptor complex negatively regulates P2X7 receptors. *J Biol Chem* 2003; 278: 37344–37351.
34. Appel CK, Gallego-Pedersen S, Andersen L, Blancheflor Kristensen S, Ding M, Falk S, Sayilekshmy M, Gabel-Jensen C and Heegaard A-M. The Src family kinase inhibitor dasatinib delays pain-related behaviour and conserves bone in a rat model of cancer-induced bone pain. *Sci Rep* 2017; 7: 4792.
35. Katsura H. Activation of Src-family kinases in spinal microglia contributes to mechanical hypersensitivity after nerve injury. *J Neurosci Off J Soc Neurosci* 2006; 26: 8680–8690.
36. Zhao Y-L, Takagawa K, Oya T, Yang H-F, Gao Z-Y, Kawaguchi M, Ishii Y, Sasaoka T, Owada K, Furuta I and Sasahara M. Active Src expression is induced after rat peripheral nerve injury. *Glia* 2003; 42: 184–193.
37. Miller WT. Determinants of substrate recognition in non-receptor tyrosine kinases. *Acc Chem Res* 2003; 36: 393–400.
38. Onofri F, Messa M, Matafora V, Bonanno G, Corradi A, Bachi A, Valtorta F and Benfenati F. Synapsin phosphorylation by SRC tyrosine kinase enhances SRC activity in synaptic vesicles. *J Biol Chem* 2007; 282: 15754–15767.
39. Chen M-L, Cao H, Chu Y-X, Cheng L-Z, Liang L-L, Zhang Y-Q and Zhao Z-Q. Role of P2X7 receptor-mediated IL-18/IL-18R signaling in morphine tolerance: multiple glial-neuronal dialogues in the rat spinal cord. *J Pain* 2012; 13: 945–958.
40. Clark AK, Wodarski R, Guida F, Sasso O and Malcangio M. Cathepsin S release from primary cultured microglia is regulated by the P2X7 receptor. *Glia* 2010; 58: 1710–1726.
41. de Torre-Minguela C, Barberà-Cremades M, Gómez AI, Martín-Sánchez F and Pelegrín P. Macrophage activation and polarization modify P2X7 receptor secretome influencing the inflammatory process. *Sci Rep* 2016; 6: 22586.
42. Lister MF, Sharkey J, Sawatzky DA, Hodgkiss JP, Davidson DJ, Rossi AG and Finlayson K. The role of the purinergic P2X7 receptor in inflammation. *J Inflamm* 2007; 4: 5.
43. Ji R-R and Suter MR. p38 MAPK, microglial signaling, and neuropathic pain. *Mol Pain* 2007; 3: 33.
44. Kawasaki Y, Zhang L, Cheng J-K and Ji R-R. Cytokine mechanisms of central sensitization: distinct and overlapping role of interleukin-1beta, interleukin-6, and tumor necrosis factor-alpha in regulating synaptic and neuronal activity in the superficial spinal cord. *J Neurosci* 2008; 28: 5189–5194.
45. Wang W-Y, Tan M-S, Yu J-T and Tan L. Role of pro-inflammatory cytokines released from microglia in Alzheimer's disease. *Ann Transl Med* 2015; 3: 136.
46. Olmos G and Lladó J. Tumor necrosis factor alpha: a link between neuroinflammation and excitotoxicity. *Mediators Inflamm* 2014; 2014: 861231.